NUCLEAR REACTIONS INDUCED IN TANTALUM BY PROTONS OF ENERGY UP TO 84 MEV[1]

C. L. RAO[2] AND L. YAFFE
Radiochemistry Laboratory, Department of Chemistry, McGill University, Montreal, Que.
Received April 19, 1963

ABSTRACT

Nuclear reactions induced in tantalum by protons of energy up to 84 Mev have been studied and excitation functions obtained for products formed by (*p*,*xn*), (*p*,*pxn*), (*p*,2*pxn*), and (*p*,3*pxn*) reactions. Radiation characteristics of the products were redetermined. Previously unreported γ-rays with energies 90 to 1050 kev have been found for W^{176}, and 113 kev for W^{177}. A new half-life of 2.7 ± 0.1 hr for W^{176} is reported. The cross sections for the (*p*,*xn*) reactions were compared with the values predicted by Jackson's schematic model and found to be in reasonable agreement. More complex reactions are discussed in the light of current nuclear theories.

INTRODUCTION

Nuclear reactions induced by protons and other particles of kinetic energies up to a few tens of Mev in medium heavy-weight elements have been chiefly interpreted in terms of the compound nucleus (1). However, significant deviations from the predictions of this model, as observed in the large inelastic scattering cross sections and the anisotropy of the emitted particles, prompted the introduction of a direct interaction mechanism (2, 3) as an alternative to the compound nucleus mechanism. The investigation of the excitation functions of a neutron-excess nucleus with high atomic number offers a convenient method of differentiating reactions that proceed through compound nucleus formation from those reactions, like (*p*,*pn*), which take place via other non-compound-nucleus processes.

The present study pertains to the investigation of the nuclear reactions induced in tantalum by protons in the energy range 8–84 Mev. In this energy range, these reactions are not greatly complicated by fission or other exotic processes. Tantalum was chosen for this study for the following reasons:

(1) The element is available in a very pure form commercially as a foil in different thicknesses, and it is essentially monoisotopic.

(2) The detailed study of the spallation reactions in this mass region ($150 < A < 200$) and energy range (8–90 Mev) is not extensive. A literature survey is given by Miller and Hudis (4) covering the work carried out up to 1959. At higher energies nuclear reactions on tantalum have been studied, among which the studies with 340 Mev (5) and 5.7 Bev (6) protons are the most comprehensive. An extension of these data to lower energies would be informative.

(3) It was also felt desirable to investigate the gamma spectra of neutron-deficient nuclides of W, Ta, Hf, and Lu, since these are poorly identified.

Even though a large number of stable nuclides would be formed in several reactions on tantalum, which cannot be studied radiochemically, a limited comparison with the total reaction cross section, as derived from the continuum theory or from the optical model, can be obtained at a few energies.

[1]*This work received financial assistance from the National Research Council of Canada.*
[2]*Present address: Radiochemistry and Isotope Division, Atomic Energy Establishment, Trombay, Bombay, India.*

Can. J. Chem. Downloaded from cdnsciencepub.com by 94.2.227.55 on 05/31/21
For personal use only.

EXPERIMENTAL PROCEDURES

(a) Target Assembly

Tantalum metal, used as the target foil, was available in two thicknesses (84.3 mg/cm² and 21 mg/cm²). The thinner foil was used in the study of (*p*,*xn*) and (*p*,*pxn*) reactions and the thicker foil for the study of (*p*,2*pxn*) and (*p*,3*pxn*) reactions.* Spectrographic analysis of the tantalum foil indicated that no detectable impurities would cause any interference in the present study. The monitor foil was a 'spec pure' copper foil 0.002 in. thick obtained from Johnson, Matthey and Co. A study to determine the recoil losses in the monitor foil was made by irradiating a copper foil and a pure aluminum foil as a catcher foil at two energies, 50 Mev and 85 Mev. The recoil losses of Cu^{64} were found to be less than 0.25% of the total Cu^{64} activity at both the above energies and were therefore neglected. The recoil losses from tantalum were not measured and it was assumed that they would be negligible. Hence no guard foils were used for the monitor or target foil during irradiations.

The tantalum foils were cleaned with concentrated nitric acid and rinsed with distilled water. The copper foils were cleaned with acetone and distilled water. The two foils, each of about 2 cm² in area, were carefully aligned and fixed to the target holder in such a way that the beam of protons first struck the monitor foil. It was necessary to ensure that equal areas of the monitor and the target foils intercepted the beam. Before bombardments, the sides of the foils were trimmed with a pair of scissors and examined under a magnifying glass to make sure that the foils were uniformly cut and the leading edge was perfectly aligned. After bombardments, the foils were again sheared at about 4 mm from the leading edge, such that, after being weighed, equal areas of the target and monitor foils were processed for activity determination.

(b) Irradiations

The target holder was fixed to the probe of the McGill Synchrocyclotron and the probe set at the desired radii, thus letting the target intercept the internal circulating proton beam at various energies. The calibration curve for radial distance vs. proton energy by Kirkaldy (7) was used. Energy degradation of the proton beam at all energies at which irradiations were carried out was estimated from the range-energy values of Sternheimer (8) and was found to be negligible within the energy spread of the proton beam (~2 Mev). The irradiation period was about one hour in most of the experiments.

(c) Chemical Procedures

The elements that are expected to be formed in the spallation of Ta in the present study are W, Ta, Hf, Lu, and possibly Yb. Depending upon the energy of the bombardment, either all or some of these elements would be formed. The formation of any product formed by secondary reactions was neglected on account of the thin targets employed in this work. In copper, zinc, copper, nickel, cobalt, and iron would be formed as spallation products. It was found convenient to separate in one series of experiments throughout the energy range only Ta and W, and in another series Hf and Lu, from the spallation products of Ta. The formation of Yb was neglected. The existing chemical procedures for the separation of the spallation products of Ta (5) and Cu (9) were slightly modified to suit the present experimental conditions in order to achieve a high degree of decontamination.† Tantalum was dissolved in the minimum amount of concentrated nitric and hydrofluoric acids in the presence of W, Zr (for Hf), and La (for Lu) carriers in a platinum crucible by gently warming the mixture on a steam bath for a few minutes. Briefly, Ta was separated by extraction with diisopropylketone from the acid medium twice, and finally back-extracted from the ketone layer into 50% tartaric acid solution. Tungsten was precipitated as $CoWO_4$ followed by complexing with thiocyanate and recovery of the tungsten in ammoniacal solution. Similarly, zirconium, used as a carrier for Hf, was precipitated as barium zirconyl fluoride and later extracted with TTA in xylene and, finally, Zr(Hf) was recovered in 5 *M* hydrochloric acid. Lanthanum, used as carrier for Lu, was precipitated as fluoride and later as hydroxide, and finally recovered in 4 *M* hydrochloric acid. Copper was separated from its spallation products by suitable adaptation of anion exchange methods.

All the solutions containing the purified elements were made up to a certain volume, and an aliquot of each was pipetted into a standard screw-cap glass vial in order to measure the radiation characteristics and decay rates. Aliquots of the above solutions were analyzed spectrophotometrically for chemical yield determinations; Ta as a phenylfluorone complex (10), W as a thiocyanate complex (11), Zr (Hf) as a thoron complex (12), La (Lu) as an alizarin red S complex (11), and Cu as diethyldithiocarbamate complex (13).

(d) Beam Intensity Measurement

In order to measure the absolute cross sections, it was necessary to know the number of protons that had passed through the target foils. Copper was used as the monitor foil for the proton beam. For low-energy bombardments, the monitor reaction $Cu^{63}(p,n)Zn^{63}$ was utilized, and the cross-section values from the excitation function given by Ghoshal (14) for this reaction were used. At higher energies (above 15 Mev),

**The nomenclature used in indicating all these reactions is not intended to imply any particular reaction mechanism.*

†*A detailed account of the chemical procedures, measurement techniques, and resolution of decay curves may be found in the thesis of Lakshman Rao Chervu, McGill University, Montreal, Que., 1962.*

Can. J. Chem. Downloaded from cdnsciencepub.com by 94.2.227.55 on 05/31/21
For personal use only.

the reaction $Cu^{65}(p,pn)Cu^{64}$ was utilized, for which the cross-section values were obtained from Meadows (15). The cross sections for the monitors at the various energies are given in Table I.

TABLE I

Monitor cross-section values used in this work

Proton energy (Mev)	σ (millibarn)		Proton energy (Mev)	σ (millibarn)	
	Zn^{63} (14)	Cu^{64} (15)		Zn^{63} (14)	Cu^{64} (15)
8	260	—	42	—	315
12	540	—	48	—	280
18	—	155	54	—	260
24	—	520	64	—	230
30	—	440	74	—	217
36	—	360	84	—	183

(e) Activity Measurements

All the samples were measured by a calibrated 3 in.×3 in. sodium iodide crystal (16) coupled to a photomultiplier tube in conjunction with a 100-channel pulse-height analyzer. This γ-ray spectrometer was used for the measurement of the intensity of γ-rays and *K* X-rays in every sample. The energy calibration was made with a number of well-known γ-ray emitters.

(f) Treatment of Data

The areas of the prominent photopeaks were converted into photon-emission rates by applying the photopeak counting efficiency in the crystal and the resolution losses as observed on the pulse analyzer. A plot of the photon-emission rate as a function of time gave the radioactive decay curve. The *K* X-ray photopeak decay curves of the samples were graphically analyzed into several components, depending upon the energy at which the irradiation was made, in order to separate the contributions from the different isotopes of each element. In those cases where some of the decaying species had radioactive daughter species growing in the fraction after radiochemical purification, graphical analysis of the multicomponent decay curve was too difficult. If an easily observed γ-ray of known energy and abundance was emitted by the parent or its daughter, the photon-emission rate of the species was obtained without resolving the *K* X-ray decay curve for that particular nuclide. In those cases where it was not possible to follow any specific γ-ray, the *K* X-ray decay curve was analyzed for the longer-lived daughter components only, from which the parent activities were estimated.

For the calculation of the disintegration rates at the end of bombardment for each nuclide observed, the corrections applied to the photon-emission rates were the following: decay during the period between the end of bombardment and the measurement time, chemical yield of the sample and dilution factor, γ-ray and *K* X-ray abundance (17, 18) per disintegration of each nuclide detected. In the case of positron emitters, the intensity of the annihilation γ-rays was measured and a factor of 2 included in the calculation of disintegration rates to allow for the emission of two quanta.

Finally, the cross sections for the formation of the nuclide were calculated by means of the following equation:

$$\sigma_p = \sigma_m \cdot \frac{D_0^p}{D_0^m} \cdot \frac{n_m}{n_T} \cdot \frac{(1-e^{-\lambda_m t})}{(1-e^{-\lambda_p t})}$$

where σ_p and σ_m = formation cross sections of product and monitor respectively;
D_0^p and D_0^m = disintegration rates of product and monitor respectively at end of bombardment;
n_m and n_T = number of atoms of monitor and target respectively;
λ_m and λ_p = disintegration constants of monitor and product respectively;
t = time of irradiation.

In the case of those nuclides which are not shielded, if the parent half-lives and formation cross sections are known, corrections for the formation from the precursors was applied to obtain independent cross sections; when the precursor half-lives are too short that they decayed away into the daughter nuclide before any chemical separation was effected, cumulative cross sections only were given.

RESULTS

*(a) Radiation Characteristics**

(i) W^{176}

This nuclide has previously been reported only by Wilkinson (19), who assigned a half-life of 80 min to it and a γ-ray of about 1.3 Mev in energy. In the present work two

**The error in gamma-ray energy values quoted is ±5% unless otherwise indicated.*

Can. J. Chem. Downloaded from cdnsciencepub.com by 94.2.227.55 on 05/31/21
For personal use only.

γ-rays of energies 90 kev and 1050 kev were found attributable to W^{176}. They decayed with a half-life of 2.7±0.1 hr over four half-lives. The mass assignment was made both on the basis of excitation functions for the $Ta^{181}(p,6n)$ reaction and the observed growth of the Ta^{176} daughter (half-life 8 hr) which was consistent with having a 2.7-hr parent.

(ii) W^{177}

This nuclide was produced by the reaction $Ta^{181}(p,5n)$. It had previously been reported only by Wilkinson (19), who found a half-life of 2.17±.05 hr for it and assigned γ-rays of energies 450 and 1200 kev to it. In the present work we found γ-rays of 113, 450, and 1050 kev decaying with a half-life of 2.2±0.1 hr over five half-lives.

(iii) W^{178}, W^{179}, W^{181}

These nuclides were prepared by the $(p,4n)$, $(p,3n)$, and (p,n) reactions respectively on Ta^{181}. The half-lives found, viz. 22±0.5 days, 40±2 min, 140±2 days, agreed well with the literature values (17). The values were derived by resolution of the X-ray curves. Ta^{178} (9.3-min half-life), in secular equilibrium with W^{178}, has a prominent γ-ray at 1.35 Mev energy and 511 kev annihilation radiation due to a 2% positron branching. Both decayed with the 22-day parent half-life.

(iv) Ta^{173}

This nuclide was produced by the $(p,p8n)$ reaction on Ta^{181} and by decay of the short-lived W^{173} formed by the $(p,9n)$ reaction on Ta^{181}. The half-life for Ta^{173} was found to be 3.7 hr, in agreement with that reported by Faler and Rasmussen (20). Ta^{173} was observed by the growth of an intense photopeak due to Hf^{173} (24 hr) in the separated tantalum fraction. Harmatz *et al.* (21) have proposed a half-life of 2.5 hr for Ta^{173}. In Fig. 1 are

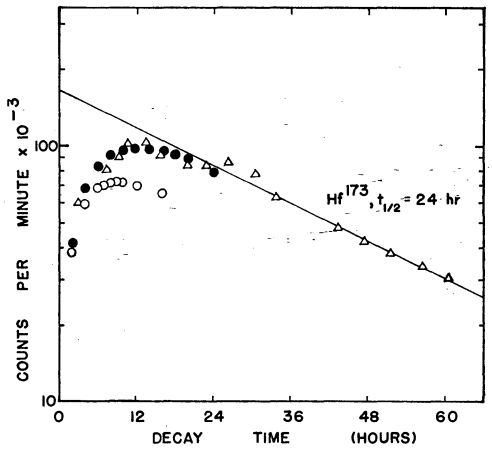

FIG. 1. Growth of 24-hr Hf^{173} from Ta^{173}: △ experimental points; ● theoretical growth curve assuming a half-life of 3.7 hr for Ta^{173}; ○ theoretical growth curve assuming a half-life of 2.5 hr for Ta^{173}.

shown the experimental data and the theoretical growth curves for both a 2.5-hr and a 3.7-hr parent feeding a 24-hr daughter. The data are consistent with the latter value.

(v) Ta^{174}

This nuclide was formed by the reaction $Ta^{181}(p,p7n)$ and by decay of short-lived W^{184} produced by the reaction $Ta^{181}(p,8n)$. The 511-kev annihilation radiation peak decayed with a half-life of 1.3±0.1 hr, in agreement with that found by Faler and Rasmussen (20).

Can. J. Chem. Downloaded from cdnsciencepub.com by 94.2.227.55 on 05/31/21
For personal use only.

(vi) Ta^{175}

The formation of this nuclide was recognized by the growth of the characteristic 340 kev γ-ray due to Hf^{175}. Gamma rays of energies 125, 205, 265, and 350 kev were found attributable to Ta^{175}. Due to the complexity of the spectrum, the abundance of Ta^{175} was calculated from the growth of Hf^{175}.

(vii) Ta^{176}

This is produced by decay of W^{176} and from the reaction $Ta^{181}(p,p5n)$. Gamma rays at 202, 1160, and 1700 kev were observed to decay with a half-life of 8 hr, in agreement with previous work. In all, about 60 transitions of energies up to 2 Mev (21) have been reported for this nuclide. The resolution of the decay curve yielded an 8-hr component, a mixture of Ta^{176} and Ta^{180m}, and thus no yield determinations of Ta^{176} were made.

(viii) Ta^{177}

This is produced by the decay of W^{177} and from the reaction $Ta^{181}(p,p4n)$. Resolution of the X-ray curves gave a half-life of 56 ± 1 hr for this nuclide, in good agreement with the work of Mann *et al.* (22).

(ix) Ta^{178}

This nuclide was formed by the reaction $Ta^{181}(p,p3n)$. Gamma rays of energies 213, 330, and 427 kev were found decaying with a half-life of 2.2 ± 0.1 hr. These γ-rays originate (17) mainly from the 4.8-sec Hf^{178m} state in equilibrium with Ta^{178}.

(x) Ta^{179}

This was formed from the reaction $Ta^{181}(p,p2n)$ and by decay of W^{179}. No prominent γ-rays were observed and measurements were made by resolution of the X-ray photopeak. A half-life of about 600 days (19) has been reported for Ta^{179}. Measurements made over a period of one half-life were consistent with this value.

(xi) Ta^{180m}

The formation cross section of this nuclide, produced by the reaction $Ta^{181}(p,pn)$, was measured by the X-ray photopeak. A half-life of 8.1 ± 0.1 hr was obtained, in good agreement with previous data (17). At higher energies, production of Ta^{176} made measurements in this fashion impossible.

(xii) Hf^{171}

The γ-ray spectrum of separated Hf fractions at higher energies was very complex. Gamma rays at 680, 880, and 1100 kev were found attributable to Hf^{171} as these were not found at bombarding energies where Hf^{173} alone was produced. Although the spectrum was too complex for decay-curve analysis, the decay of these peaks was consistent with a 16-hr half-life (17). The growth of the 740 kev photopeak due to the Lu^{171m} daughter (21) was used to measure the formation cross section.

(xiii) Hf^{172}

This nuclide (half-life $\sim$ 5 yr) was identified and measured with the help of the high-energy photopeaks due to Lu^{172} (6.7 day) in secular equilibrium with the parent nuclide.

(xiv) Hf^{173}

Very intense photopeaks at 120 and 300 kev decayed with a half-life of 24 ± 0.5 hr. This nuclide was observed both as a direct spallation product and, at high energies, by decay of its precursors.

(xv) Hf^{175}

The very intense 340 kev photopeak attributable to this nuclide decayed with a half-life of 70 ± 2 days. Hf^{175} was formed directly at 42 Mev proton bombarding energies.

Can. J. Chem. Downloaded from cdnsciencepub.com by 94.2.227.55 on 05/31/21
For personal use only.

This did not result from decay of Ta^{175} since the formation of the latter was not observed at proton energies less than 64 Mev. At these energies the production of Hf^{175} from its precursors was observed.

(xvi) Hf^{180m}

This nuclide was first observed at a proton bombarding energy of 42 Mev. Characteristic γ-rays at energies of 216, 340, 440, and 500 kev were found. The 216 kev peak decayed with a half-life of 5.5 ± 0.1 hr, in excellent agreement with the result of Burson *et al.* (23).

(xvii) Lu^{171m}

This was identified by the characteristic photopeak (21) at 740 kev. The decay of this photopeak gave a half-life of 7.7 ± 0.2 days, measured over a period of four half-lives, shorter than that of 8.2 days reported by Bonner *et al.* (24).

(xviii) Lu^{172}

Gamma rays at energies of 113, 180, 200, 300, 370, and 1090 kev were observed. The decay of the most intense peak was followed for seven half-lives and gave a value of 6.7 ± 0.1 days, in very good agreement with the literature values (17).

(xix) Lu^{176m}

The decay of the 90 kev gamma peak reported (17) for this nuclide gave a half-life of 3.8 hr, in good agreement, with literature values (17).

(xx) Lu^{177}

This was detected as a very weak β^- activity observed in lutetium fraction decaying with a half-life of approximately 7 days. The gamma spectrum indicated weak peaks at 113 and 208 kev due to Lu^{177}.

(b) Experimental Cross Sections

The radiation characteristics used to determine the formation cross sections are given in Table II. The cross sections found experimentally are listed in Table III. The estimated accuracy quoted for each cross-section value is the standard deviation calculated by

TABLE II

Radiation characteristics used to determine formation cross sections of nuclides

Nuclide	Half-life	Radiation measured	Abundance (per disintegration)
W^{181}	140 days	K X-rays	0.72 (25)
W^{179}	40 min	K X-rays	1 (assumed)
W^{178}	22 days	K X-rays	1.54 (W^{178} + Ta^{178}) (6)
W^{177}	2.2 hr	K X-rays	0.87 (calc.)
W^{176}	2.7 hr	K X-rays	0.94 (calc. for Ta^{176})
Ta^{180m}	8.1 hr	K X-rays	0.66 (26)
Ta^{179}	600 days	K X-rays	0.57 (25)
Ta^{178}	2.2 hr	K X-rays	1 (17)
Ta^{177}	56 hr	K X-rays	0.87 (6)
Ta^{175}	11 hr	340 kev γ (Hf^{175})	0.86 (17)
Ta^{174}	1.3 hr	511 kev γ	0.76 (20)
Ta^{173}	3.7 hr	120 kev γ (Hf^{173})	1.1 (17)
Hf^{180m}	5.5 hr	216 kev γ	0.88 (17)
Hf^{175}	70 days	340 kev γ	0.86 (17)
Hf^{173}	24 hr	120 kev γ	1.1 (17)
Hf^{172}	5 yr	1.09 Mev γ (Lu^{172})	0.61 (17)
Hf^{171}	16 hr	740 kev γ (Lu^{171m})	1 (21)
Lu^{177}	6.7 days	β^-	1 (17)
Lu^{176m}	3.8 hr	390 kev γ	0.13 (estimated)
Lu^{172}	6.7 days	1.09 Mev γ	0.61 (17)
Lu^{171m}	7.7 days	740 kev γ	1 (21)

Can. J. Chem. Downloaded from cdnsciencepub.com by 94.2.227.55 on 05/31/21
For personal use only.

Can. J. Chem. Downloaded from cdnsciencepub.com by 94.2.227.55 on 05/31/21
For personal use only.

TABLE III

Formation cross sections

	Proton energy (Mev):													
	8	12	18	24	30	36	42	48	54	64	74	84	Type of yield	Accuracy (%)
	σ (millibarn)													
Nuclide														
W^{181}	60	98	35	47	44								I	±22
W^{179}			26	1200	920	280							I	±22
W^{178}					240	760	430	200	130	120	62	64	I	±22
W^{177}						130	550	830	650	200	110	98	I	±28
W^{176}								87	420	320	170	73	I	±28
Ta^{180m}			16	100	110	180	170						I	±22
Ta^{179}			0.5	29	74	190							I	±28
Ta^{178}						38	82	180	180				I	±28
Ta^{177}						5	120	280	270	170	180	220	I	±28
Ta^{175}										130	440	290	C	±28
Ta^{174}												300	C	±28
Ta^{173}												160	C	±28
Hf^{180m}							0.03		.05				I	±28
Hf^{175}							6		13	10	3	2	I	±28
Hf^{173}										25	21	24	I	±28
Hf^{172}											22		C	±28
Hf^{171}											3.5	21	C	±28
Lu^{177}							0.05						I	±28
Lu^{176m}							0.008		.08	0.2			I	±22
Lu^{172}										.07	1.2	3.7	I	±22
Lu^{171m}											0.3	2.6	I	±28

NOTE: I = independent yield; C = cumulative yield.

taking into account the errors in obtaining the disintegration rates and saturation factors. No allowance was made for the uncertainty in the monitor cross-section values or for that in the radiation abundance values used.

DISCUSSION

The formation cross sections presented in Table III indicate the general behavior expected in the spallation of a medium-weight element, in the energy range 8–84 Mev, namely production of neutron-deficient nuclides up to of the order of a few mass numbers below that of the target nucleus.

(a) (p,xn) Cross Sections

The individual excitation functions for the (*p,xn*) reactions, forming W isotopes, all exhibit sharp peaks separated from each other by about 12 Mev, as shown in Figs. 2–6.

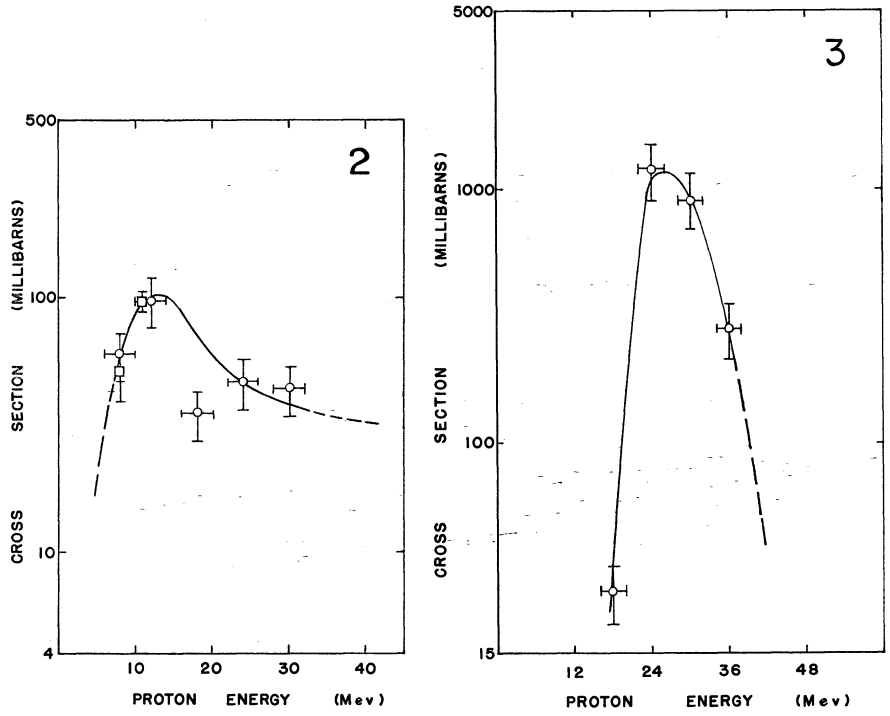

FIG. 2. Excitation function for the $Ta^{181}(p,n)W^{181}$ reaction: ○ present work; □ Hansen *et al.* (34).
FIG. 3. Excitation function for the $Ta^{181}(p,3n)W^{179}$ reaction.

These are typical of reactions proceeding at lower energies through the formation of a compound system with the subsequent decay governed by statistical considerations. The tailing off of each of these excitation functions at higher energies indicates that the nucleon–nucleon internal cascade mechanism (27) is becoming important.

In order to calculate the cross section for the (*p,xn*) reaction proceeding primarily through a compound nucleus mechanism in heavy non-fissile elements at these energies, an application of the statistical model was made by Jackson (28). He combined the Monte Carlo calculations of McManus *et al.* (29) for the prompt knock-on cascade process with a simplified evaporation model in order to calculate the excitation functions for the

Can. J. Chem. Downloaded from cdnsciencepub.com by 94.2.227.55 on 05/31/21
For personal use only.

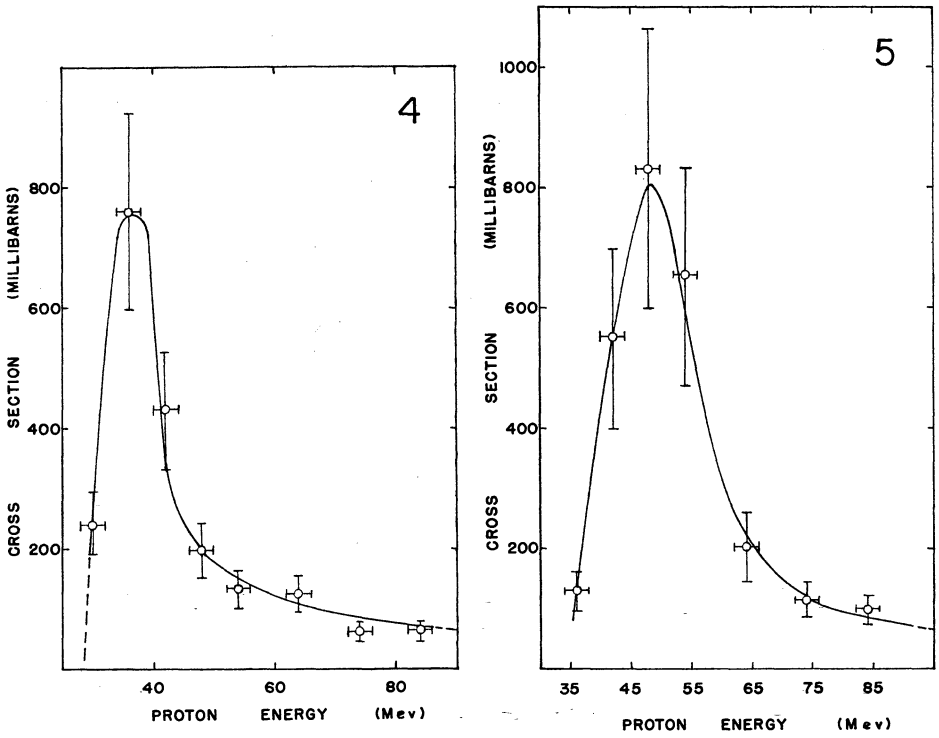

FIG. 4. Excitation function for the $Ta^{181}(p,4n)W^{178}$ reaction.
FIG. 5. Excitation function for the $Ta^{181}(p,5n)W^{177}$ reaction.

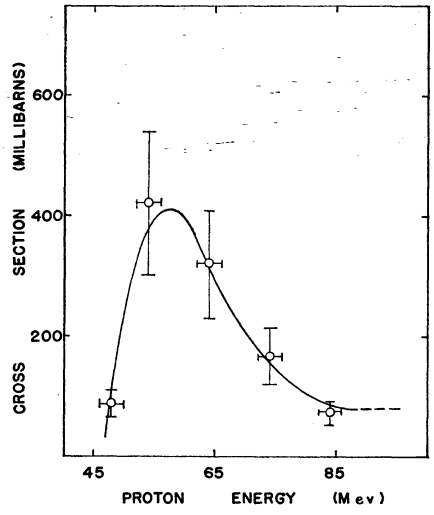

FIG. 6. Excitation function for the $Ta^{181}(p,6n)W^{176}$ reaction.

(p,xn) reaction up to 100 Mev. In the energy range up to 50 Mev, the knock-on cascade process enters as a minor correction, since the incident protons that enter the nuclear core will probably lead to compound nucleus formation. Hence the Jackson model was applied in the present work assuming only the compound nucleus mechanism.

Can. J. Chem. Downloaded from cdnsciencepub.com by 94.2.227.55 on 05/31/21
For personal use only.

The probability that a nucleus with initial excitation energy E will evaporate exactly x neutrons is given by:

$$P(E,x) = I(\Delta_x,2x-3)-I(\Delta_{x+1},2x-1),$$

where $I(z,n)$ is Pearson's incomplete gamma function,

$$\Delta_x = (E - \textstyle\sum_i^x B_i)/T.$$

B_i is the binding energy of the ith neutron, and Δ_x is the energy (in units of T, the nuclear temperature) above the threshold for the emission of x neutrons. The nuclear temperature is given by the relationship

$$\Delta E = \bar{B}+2T.$$

ΔE in Mev is the energy separation between the successive peaks of the (p,xn) excitation functions (12 Mev) which corresponds closely to the average energy carried off by the successive neutrons. $\bar{B}$, the average neutron binding energy, was calculated as 8.1 Mev from the neutron binding energies given by Seeger (30). A nuclear temperature of 1.95 Mev was thus deduced. The $P(E,x)$ values for several values of x were obtained from Pearson's Incomplete Gamma Function Tables (31) and individual neutron binding energies from Seeger's Mass Tables.

If the mechanism is assumed to be entirely that of compound nucleus formation, then

$$\sigma(p,xn) = \sigma_c(E_0)P(E,x),$$

where $\sigma_c(E_0)$ is the cross section for compound nucleus formation at an incident proton energy of E_0. The values of $\sigma_c(E_0)$ were calculated from the continuum theory of Shapiro (32) for a nuclear radius of $R = 1.3\times10^{-13}\ A^{1/3}$cm. The experimental and calculated excitation functions are given in Fig. 7.

As is evident from the results, the agreement is good only at some energies for all the reactions. The theoretical curves fall slightly to the right of those experimentally determined. A smaller value for the nuclear temperature would shift the predicted curves to slightly lower energies, but that alone would not give any better agreement with the experimental values. A more detailed account of the properties of the nucleus, combined with the excitation distribution appropriate to each of the prompt processes and evaporation steps, would perhaps better predict these cross-section values.

A comparison with the (p,xn) excitation functions (33) for Bi and Pb with those of Ta shows that the Ta curves are shifted to lower energies, since the incident proton binding energy is 6.6 Mev for Ta^{181} as compared to 5 Mev for Bi^{209} and 3.3 Mev for Pb^{206}. At low energies, at 8 Mev and 12 Mev, the cross section for the (p,n) reaction reported here, 60 and 98 millibarns respectively, are comparable to the values given by Hansen *et al.* (34) for the same reaction, 52 and 90 millibarns at the corresponding energies. At the highest bombarding energy, 84 Mev, the cross-section values for $(p,4n)$, $(p,5n)$, and $(p,6n)$ reactions are 64, 98, and 73 millibarns as compared to the values for these reactions at 340 Mev by Nervik and Seaborg (5), which are 65, 30, and 65 millibarns. The cross section for the $(p,6n)$ reaction product W^{176} by Nervik and Seaborg will be nearly halved in view of the new half-life of 2.7 hr reported for this nuclide in the present work as compared to the earlier value of 1.3 hr.

(b) (p,pxn), (p,2pxn), and (p,3pxn) Cross Sections

The data for the (p,pxn) reactions are shown in Figs. 8–11. The excitation functions

Can. J. Chem. Downloaded from cdnsciencepub.com by 94.2.227.55 on 05/31/21
For personal use only.

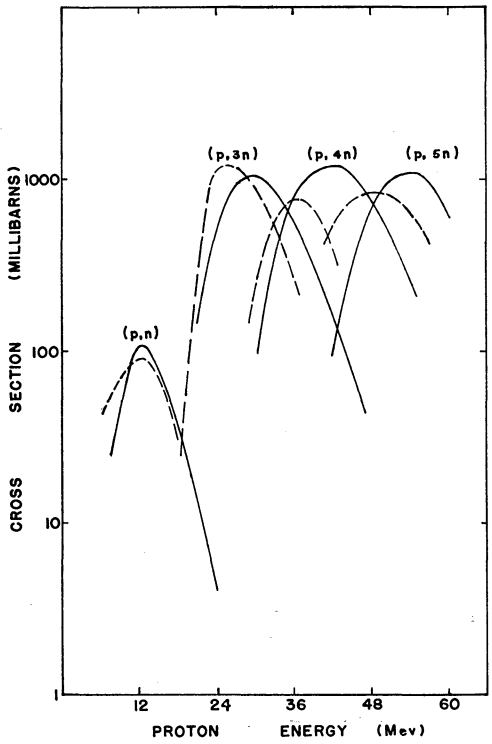

FIG. 7. Comparison of experimental excitation functions with those predicted by the Jackson model: - - - experimental; — Jackson model.

of these reactions, as well as the more complex ones, increase rapidly above the threshold. Some of these reach a maximum value and then decrease slowly with increasing energy, while others increase monotonically up to the highest bombarding energy (84 Mev). Reactions of this type are expected to have negligibly small cross sections compared with the (*p*,*xn*) cross section in medium-heavy target nuclei like Ta on the basis of statistical theory, since they are inhibited by the Coulomb barrier in both the entrance and exit channels. The experimental cross sections for these reactions are, however, quite large and the alternative mechanism proposed, that might lead to these reactions at low and medium energies, is the direct interaction (2, 3) process. The difference between the direct interaction mechanism at low energies and at high energies proposed by Serber (27) is that at low energies the knock-on process is assumed to occur with the nucleons in the surface of the target nucleus, while at higher energies direct interaction occurs in the interior of the nucleus with a sharp boundary. Internal direct processes at low energies account for only a very small fraction of the (*p*,*xpxn*) cross sections and hence are relatively unimportant (28, 35). Monte Carlo calculations of the cascade–evaporation phases of the high-energy interactions (35–38), based on the Serber model, assume a sharp cutoff nuclear boundary, and the cross sections predicted (26, 39) for the (*p*,*xpxn*) reactions at high energies are smaller than the experimental values. Further, these calculations do not take into account any interaction in the knock-on phase with the incoming particle of aggregates of nucleons and thus cascade emission of complex units as deuterons, tritons, or alphas is neglected. In the light of these remarks, the spallation yields of (*p*,*xpxn*) reactions on Ta are discussed below in the order of increasing complexity.

Can. J. Chem. Downloaded from cdnsciencepub.com by 94.2.227.55 on 05/31/21
For personal use only.

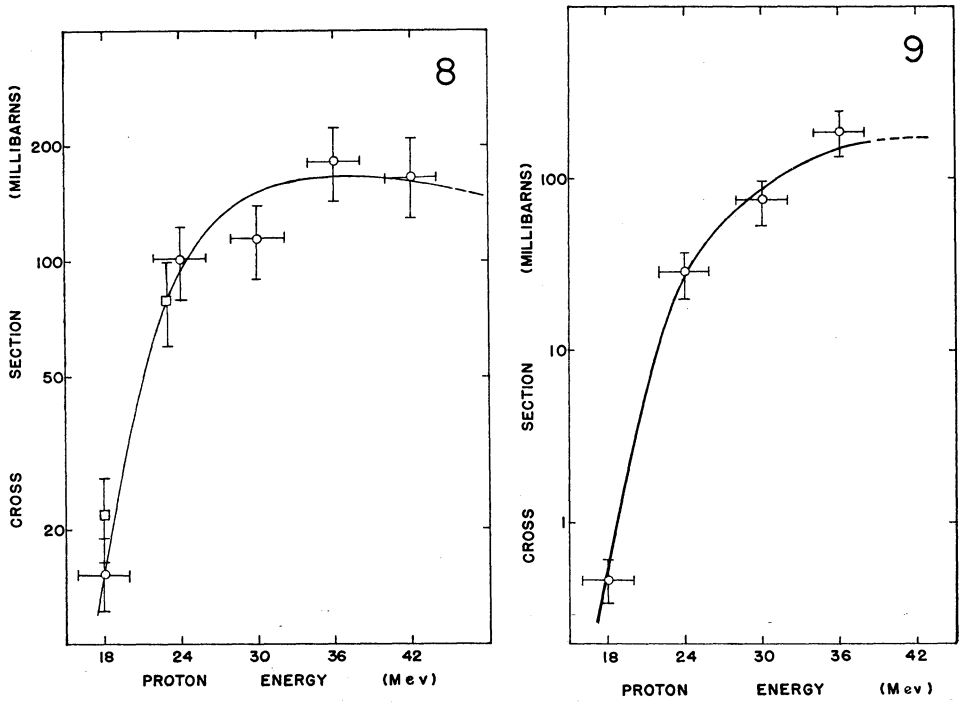

FIG. 8. Excitation function for the $Ta^{181}(p,pn)Ta^{180m}$ reaction: ○ present work; □ Cohen *et al.* (43).
FIG. 9. Excitation function for the $Ta^{181}(p,p2n)Ta^{179}$ reaction.

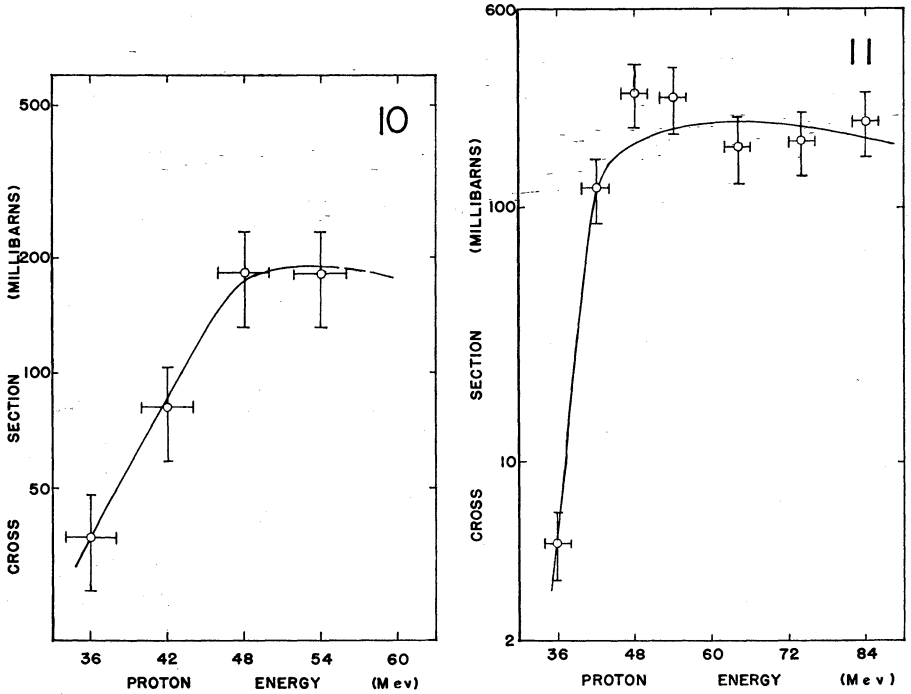

FIG. 10. Excitation function for the $Ta^{181}(p,p3n)Ta^{178}$ reaction.
FIG. 11. Excitation function for the $Ta^{181}(p,p4n)Ta^{177}$ reaction.

Can. J. Chem. Downloaded from cdnsciencepub.com by 94.2.227.55 on 05/31/21
For personal use only.

(i) (p,pn) and (p,2p) Cross Sections

These two reactions lead partially to isomeric states and partially to the stable ground states of Ta^{180} and Hf^{180} respectively. It is not known what percentage goes to the ground states and hence any comparison of cross sections for Ta^{180m} and Hf^{180m} indicates only the nature of the reaction paths favoring one reaction over the other. The possible mechanisms for these two reactions in this energy range are:

(*a*) direct interaction process involving collision of the incident proton with a neutron or a proton in which both collision partners escape from the nucleus;

(*b*) direct inelastic scattering of the incident proton followed by evaporation of a particle;

(*c*) for the (*p,pn*) reaction, the emission of deuterons by the well-known pickup process, i.e. the (*p,d*) reaction, which is another case of direct interaction important at low energies.

A comparison of the cross section for the (*p,2p*) reaction forming Hf^{180m} at 42 Mev, 0.03 millibarn, with the cross section for the (*p,pn*) reaction forming Ta^{180m} at the same energy, 170 millibarns, indicates how the several reaction paths favor the production of Ta^{180m} in contrast to that of Hf^{180m}. For the formation of Hf^{180m}, only mechanism (*a*) is significant. The fact that the cross sections for (*p,2p*) reactions below 54 Mev are extremely small is consistent with the Monte Carlo calculations (35, 36), indicating that, below about 100 Mev, absolute values of cross sections for multiple particle cascades are small. The yields for both Hf^{180m} and Ta^{180m} could not be studied up to the highest bombarding energy available. The probability for the (*p,2p*) reaction may increase due to an increase in the knock-on process, while the (*p,pn*) cross section may level off or gradually drop due to the decreasing importance of mechanism (*c*) among other factors (26, 40). The excitation function for Ta^{180m} compares well with those obtained for the same reaction on Ir^{193} reported by Grant (41) and on Au^{197} by Kavanagh and Bell (42) in the energy range where the investigations overlap. Cohen *et al.* (43) report a value of 80 millibarns at 23 Mev for the same reaction on Ta^{181}, in close agreement with the present work.

(ii) (p,p2n), (p,p3n), and (p,p4n) Cross Sections

These reactions occur by the same mechanism as discussed above. The excitation energy of the residual nucleus after the direct interaction event must be appropriate to evaporate the required number of neutrons. The pickup process, e.g. (*p,t*) reaction, may also contribute to these cross sections. After reaching a maximum cross-section value, the excitation functions level off or decrease slowly with increasing bombarding energy. The maximum cross-section values are about the same for all these reactions, including the previously discussed (*p,pn*) reaction. It may be mentioned that the Ta^{178} yield represents only a part of the $Ta^{181}(p,p3n)$ cross section, so that the yields for all these reactions are quite large.

The cross-section value for the (*p,p3n*) reaction at 54 Mev, 180 millibarns, may be compared with the cross-section value of 152 millibarns reported by Nervik and Seaborg at 340 Mev (5). The cross section for Ta^{177}, formed by the (*p,p4n*) reaction at 84 Mev, is 220 millibarns and at 340 Mev, 27 millibarns, as reported by the same authors.

(iii) (p,2pxn) and (p,3pxn) Cross Sections

The direct interaction mechanism suggested for the (*p,pxn*) reactions involving inelastic scattering of the proton followed by particle evaporation cannot possibly account for the formation yields of the (*p,2pxn*) and (*p,3pxn*) reactions observed from 42 Mev onwards with appreciable cross sections. If the direct interaction occurs with only one particle, the residual excitation energy may be insufficient to evaporate even a number of neutrons. For example, at 42 Mev, Hf^{175} formed by (*p,2p5n*) reaction has a cross section of 6.0

Can. J. Chem. Downloaded from cdnsciencepub.com by 94.2.227.55 on 05/31/21
For personal use only.

millibarns and Lu^{177} produced by the $(p,3p2n)$ reaction has a value of 0.05 millibarn. The threshold energies ($-Q$ values) calculated from Seeger's mass tables (30) for formation of these nuclides, formally written as $(p,2pxn)$ and $(p,3pxn)$ reaction products, are listed in Table IV.

TABLE IV
Threshold calculations

Product nuclide	Reaction mechanism	$-Q$ (Mev)
Hf^{175}	$(p,2p5n)$	42.7
Hf^{173}	$(p,2p7n)$	58.4
Hf^{172}	$(p,2p8n)$	64.5
Hf^{171}	$(p,2p9n)$	74.6
Lu^{177}	$(p,3p2n)$	26.7
Lu^{176}	$(p,3p3n)$	34.6
Lu^{172}	$(p,3p7n)$	63.5
Lu^{171}	$(p,3p8n)$	71.0

It has been known that the (p,α) reactions in medium heavy elements proceed through direct interaction of the incoming proton with an alpha particle or by a triton pickup reaction (44, 45). This process must be assumed to occur only at the nuclear surface, instead of throughout the nuclear volume, because of the small mean free path of the α-particles in nuclear matter (46). A nucleon, in the peripheral region of the nucleus, spends a substantial fraction of its time, probably about one-third to one-half, in an 'alpha particle' as concluded by Hodgson (45) at 40 Mev and at higher energies by Ostroumov and Filov (47). The (p,α) cross section in Ta^{181} at 23 Mev is 6 millibarns (48) and it probably increases at higher energies. According to Lindner and Turkevich (39), the yields of the products of the reactions, formally written as $(p,3pxn)$, are considerably higher than predicted by the cascade–evaporation model (35, 36), and they state that such products are perhaps produced by the reaction of the $(p,\alpha pxn)$ type in which the α-particle is knocked out of the nucleus during the cascade step, since the evaporation stage seems hardly likely to provide enough charged-particle emission in heavy elements bombarded with 340 Mev proton. Similarly, at lower energies below 70 Mev, Foreman *et al.* (49) suggest that $(\alpha,xpxn)$ reactions are formed by direct interaction with complex particles emitted in preference to a series of protons and neutrons. Thus at low energies below 100 Mev, the large yields of the $(p,2pxn)$ and $(p,3pxn)$ reaction products in Ta^{181} can best be explained by direct interaction of the incoming particle with aggregates of nucleons, like H^3, He^3, He^4, He^6, Li^5, Li^6, Li^7, etc., followed by evaporation of an appropriate number of neutrons, rather than by multiple emission of particles, unless an appreciable reduction of the Coulomb barrier, proposed only at high energies of excitation (50, 51), occurs even at low excitation energies (48) permitting the evaporation of charged particles. However, it has been shown theoretically that barrier penetrability should remain roughly constant up to 30 Mev of excitation energy (52).

The $(p,2pn)$, $(p,2p2n)$, $(p,2p3n)$, and $(p,2p4n)$ reactions lead to Hf^{179}, Hf^{178}, Hf^{177}, and Hf^{176}, respectively which are stable and their yields cannot be determined radiochemically. The $(p,2p5n)$ reaction product, Hf^{175}, would probably result from a $(p,Hexn)$ reaction, with the proton–helium isotope knockout mechanism, followed by neutron evaporation at 42 Mev and above. Its isobar, Ta^{175}, formed either through the decay of W^{175} or independently through a $(p,p6n)$ reaction, was observed only at bombarding energies above 64 Mev, which might be explained on the basis that no alternative reaction paths are

Can. J. Chem. Downloaded from cdnsciencepub.com by 94.2.227.55 on 05/31/21
For personal use only.

available for its formation, except by neutron evaporation from an excited nucleus after proton inelastic scattering. It may also be pointed out that the two reaction products, Ta^{178} formed by the $(p,p3n)$ reaction and Hf^{175} produced by the $(p,\alpha 3n)$ reaction, were observed at about the same energy, the former at 36 Mev and the latter at 42 Mev, suggesting a similarity of the two reaction processes. The drop in the excitation function for Hf^{175} at higher energies is somewhat puzzling and further experiments alone would clarify this point. The independent yields of Hf^{178}, formed by the $(p,2p7n)$ reaction, may also be explained by the same mechanism of helium isotope surface knockout, followed by neutron evaporation. Its formation in comparable yield to that of Hf^{175} indicates a greater deposition of energy in the residual nucleus with increasing bombarding energy favoring evaporation of many neutrons, which may be one of the reasons for the gradual decrease in the yields of Hf^{175} at higher energies.

The $(p,3pxn)$ reaction products have been observed at about 42 Mev. The $(p,3p2n)$ reaction at 42 Mev, leading to Lu^{177}, has a low cross section, 0.05 millibarn, indicating the low probability even for its alternative reaction path, $(p,\alpha p)$ mechanism, in which both collision partners escape the target nucleus, as explained for the $(p,2p)$ reaction. Lu^{176} formed by a $(p,3p3n)$ reaction cannot be determined radiochemically, and the yield determined for Lu^{176m} represents only a fraction of the total yield for this reaction. The yields are low, 0.2 millibarn at 64 Mev, indicating the low probability for the reaction to occur via a $(p,\alpha d)$, $(p,\alpha pn)$, or (p,Li^5n) reaction, the last reaction being more probable than the others. Lu^{172} and Lu^{171m}, produced by $(p,3p7n)$ and $(p,3p8n)$ reactions at 84 Mev, have cross sections of 3.7 and 2.6 millibarns respectively, and they are likely to be formed by surface interaction with a lithium isotope or a helium isotope followed by particle evaporation.

A comparison of the cross-section values for the $(p,2pxn)$ and $(p,3pxn)$ reactions in Ta^{181} with those of similar reactions induced in erbium isotopes (53) and iridium isotopes (41) does show that the high yields for these reactions indeed occur in the medium heavy elements even in the energy range of present interest.

(c) The Total Reaction Cross Section

At low energies (<12 Mev) the measurement of the (p,xn) cross section gives direct information about the proton reaction cross section, since the contribution from the proton inelastic scattering cross section is negligible. Experimentally, it was found in the present study that the (p,pn) reaction did not occur at 12 Mev, in agreement with Cohen *et al.* (43), who determined a value of about 0.5 millibarn at 13.5 Mev for this reaction. Thus, at 8 Mev and 12 Mev, the total reaction cross section is the sum of the cross sections for (p,n) and $(p,2n)$ reactions, the others like (p,γ) being negligible. The experimentally determined values for the (p,n) reaction at 8 Mev and 12 Mev in this work are 60 and 98 millibarns. The $(p,2n)$ reaction leading to stable W^{180} has calculated (34) cross-section values of 6 and 400 millibarns at 8 Mev and 12 Mev respectively. Thus the total reaction cross-section values of 66 millibarns at 8 Mev and 500 millibarns at 12 Mev compare well with the values computed with the optical model using a surface absorption potential (34). The proton capture cross sections at these energies, calculated by Shapiro (32) with $R = 1.5\times10^{-13}A^{1/3}$, correspond to 60 and 470 millibarns, which also agree with the above total reaction cross-section values, again pointing out that the (p,n) interaction proceeds via the compound nucleus at these low energies and direct interaction interference is negligible.

The theoretical proton total reaction cross section at 31.5 Mev given by Melkanoff *et al.* (54) for Ta is 1830 millibarns, which may be compared with the value, 1650 ± 360

Can. J. Chem. Downloaded from cdnsciencepub.com by 94.2.227.55 on 05/31/21
For personal use only.

millibarns, obtained at 30 Mev in the present work. The experimental value includes the (p,p') cross section for Ta at 31 Mev (2) and also the $(p,2n)$ cross section at 30 Mev (55) for Bi^{209}. The (p,α) cross sections are not significant. A similar experimental value of 1600 millibarns was given (42) for the total reaction cross section of a medium heavy nucleus like Au^{197} or Bi^{209}. Gooding (56) reported a value of 1775 millibarns for Pb as the total proton reaction cross section at 34 Mev, obtained by beam attenuation measurements. A similar comparison cannot be extended to higher energies because of the large number of competing undetermined cross sections.

ACKNOWLEDGMENTS

The authors wish to express their appreciation to Dr. R. E. Bell for making the facilities of the Radiation Laboratory so readily available to us.

One of us (C. L. R.) wishes to express his appreciation to the Canadian Universities Foundation and to the Ministry of Scientific Research and Cultural Affairs, Government of India, under whose joint auspices a Canadian Commonwealth Scholarship was held.

REFERENCES

1. J. M. Blatt and V. F. Weisskopf. Theoretical nuclear physics. John Wiley and Sons, Inc., New York. 1952.
2. R. M. Eisberg and G. Igo. Phys. Rev. **93**, 1039 (1954).
3. N. Austern, J. T. Butler, and H. McManus. Phys. Rev. **92**, 350 (1953).
4. J. M. Miller and J. Hudis. Ann. Rev. Nucl. Sci. **9**, 159 (1959).
5. W. E. Nervik and G. T. Seaborg. Phys. Rev. **97**, 1092 (1955).
6. J. R. Grover. Phys. Rev. **126**, 1540 (1962).
7. J. S. Kirkaldy. Ph.D. Thesis, McGill University, Montreal, Que. 1953.
8. R. M. Sternheimer. Phys. Rev. **117**, 137 (1959).
9. K. A. Kraus and F. Nelson. Proc. Intern. Conf. Peaceful Uses At. Energy, Geneva, 1955, **7**, 113 (1955).
10. C. L. Luke. Anal. Chem. **31**, 904 (1959).
11. E. B. Sandell. Colorimetric determination of traces of metals. 3rd ed. Interscience Publishers, Inc., New York. 1959.
12. A. D. Horton. Anal. Chem. **25**, 1331 (1953).
13. T. D. Price and R. E. Telford. National Nuclear Energy Series. Div. VIII, Vol. 1. McGraw-Hill Book Co., Inc. New York. 1950. p. 404.
14. S. N. Ghoshal. Phys. Rev. **80**, 939 (1950).
15. J. W. Meadows. Phys. Rev. **91**, 885 (1953).
16. G. V. S. Rayudu, M. May, and G. R. Grant. Quoted in thesis of G. R. Grant, McGill University, Montreal, Que. 1961.
17. Nuclear Data Sheets. National Academy of Sciences, National Research Council (U.S. Government Printing Office, Washington, D.C.). 1959.
18. D. Strominger, J. M. Hollander, and G. T. Seaborg. Rev. Mod. Phys. **30**, 585 (1958).
19. G. Wilkinson. Phys. Rev. **80**, 495 (1950).
20. K. T. Faler and J. O. Rasmussen. Phys. Rev. **118**, 265 (1960).
21. B. Harmatz, T. H. Handley, and J. W. Mihelich. Phys. Rev. **119**, 1345 (1960).
22. L. G. Mann, R. J. Nagle, and H. I. West. Bull. Am. Phys. Soc. **2**, 231 (1957).
23. S. B. Burson, K. W. Blair, H. B. Keller, and S. Wexler. Phys. Rev. **83**, 62 (1951).
24. N. A. Bonner, W. Goishi, W. H. Hutchin, G. M. Iddings, and H. A. Tewes. Phys. Rev. **127**, 217 (1962).
25. R. C. Jopson, H. Mark, C. D. Swift, and J. H. Zenger. Phys. Rev. **124**, 157 (1961).
26. S. S. Markowitz, S. S. Rowland, and G. Friedlander. Phys. Rev. **112**, 1295 (1958).
27. R. Serber. Phys. Rev. **72**, 1114 (1947).
28. J. D. Jackson. Can. J. Phys. **34**, 767 (1956).
29. H. McManus, W. T. Sharp, and H. Gellman. Phys. Rev. **93**, 924 (1954).
30. P. A. Seeger. Nucl. Phys. **25**, 1 (1961).
31. K. Pearson. Tables of the incomplete gamma functions. Cambridge University Press, Cambridge, England. 1951.
32. M. M. Shapiro. Phys. Rev. **90**, 171 (1953).
33. R. E. Bell and H. M. Skarsgard. Can. J. Phys. **34**, 745 (1956).
34. L. F. Hansen, R. C. Jopson, H. Mark, and C. D. Swift. Nucl. Phys. **30**, 389 (1962).
35. N. Metropolis, R. Bivins, M. Storm, A. Turkevich, J. M. Miller, and G. Friedlander. Phys. Rev. **110**, 185 (1958).
36. N. Metropolis, R. Bivins, M. Storm, J. M. Miller, G. Friedlander, and A. Turkevich. Phys. Rev. **110**, 204 (1958).

Can. J. Chem. Downloaded from cdnsciencepub.com by 94.2.227.55 on 05/31/21
For personal use only.

37. I. DOSTROVSKY, P. RABINOWITZ, and R. BIVINS. Phys. Rev. **111**, 1659 (1958).
38. I. DOSTROVSKY, Z. FRAENKEL, and P. RABINOWITZ. Proc. Intern. Conf. Peaceful Uses At. Energy, Geneva, **15**, 1615 (1958).
39. M. LINDNER and A. TURKEVICH. Phys. Rev. **119**, 1632 (1960).
40. W. R. WARE and E. O. WIIG. Phys. Rev. **122**, 1837 (1961).
41. G. R. GRANT. Ph.D. Thesis, McGill University, Montreal, Que. 1961.
42. T. M. KAVANAGH and R. E. BELL. Can. J. Phys. **39**, 1172 (1961).
43. B. L. COHEN, E. NEWMAN, R. A. CHARPIE, and T. H. HANDLEY. Phys. Rev. **94**, 620 (1954).
44. C. B. FULMER and B. L. COHEN. Phys. Rev. **112**, 1672 (1958).
45. P. E. HODGSON. Nucl. Phys. **8**, 1 (1958).
46. W. B. CHESTON and A. E. GLASSGOLD. Phys. Rev. **106**, 1215 (1957).
47. V. I. OSTROUMOV and R. A. FILOV. J. Exptl. Theoret. Phys. (USSR), Translation, **10**, 459 (1960).
48. C. B. FULMER and C. D. GOODMAN. Phys. Rev. **117**, 1339 (1960).
49. B. M. FOREMAN, JR., W. M. GIBSON, R. A. GLASS, and G. T. SEABORG. Phys. Rev. **116**, 382 (1959).
50. K. J. LE COUTEUR. Proc. Phys. Soc. (London), A, **63**, 259 (1950); A, **65**, 718 (1952).
51. Y. FUJIMOTO and Y. YAMAGUCHI. Prog. Theoret. Phys. (Kyoto), **5**, 76 (1950).
52. A. M. LANE and K. PARKER. Nucl. Phys. **16**, 690 (1960).
53. G. V. S. RAYUDU. Ph.D. Thesis, McGill University, Montreal, Que. 1961.
54. M. A. MELKANOFF, J. S. NODVIK, D. S. SAXON, and R. D. WOODS. Phys. Rev. **106**, 793 (1957).
55. E. L. KELLEY. Univ. Calif. Radiation Lab. Rept. UCRL-1044. 1950. Unpublished.
56. T. J. GOODING. Nucl. Phys. **12**, 241 (1959).

Can. J. Chem. Downloaded from cdnsciencepub.com by 94.2.227.55 on 05/31/21
For personal use only.